TECHNICAL REVIEW

New Design Principle for Triaxial PZ Accelerometers

FE models for Optimizing Accelerometer Designs

High Pressure Microphone Calibration System

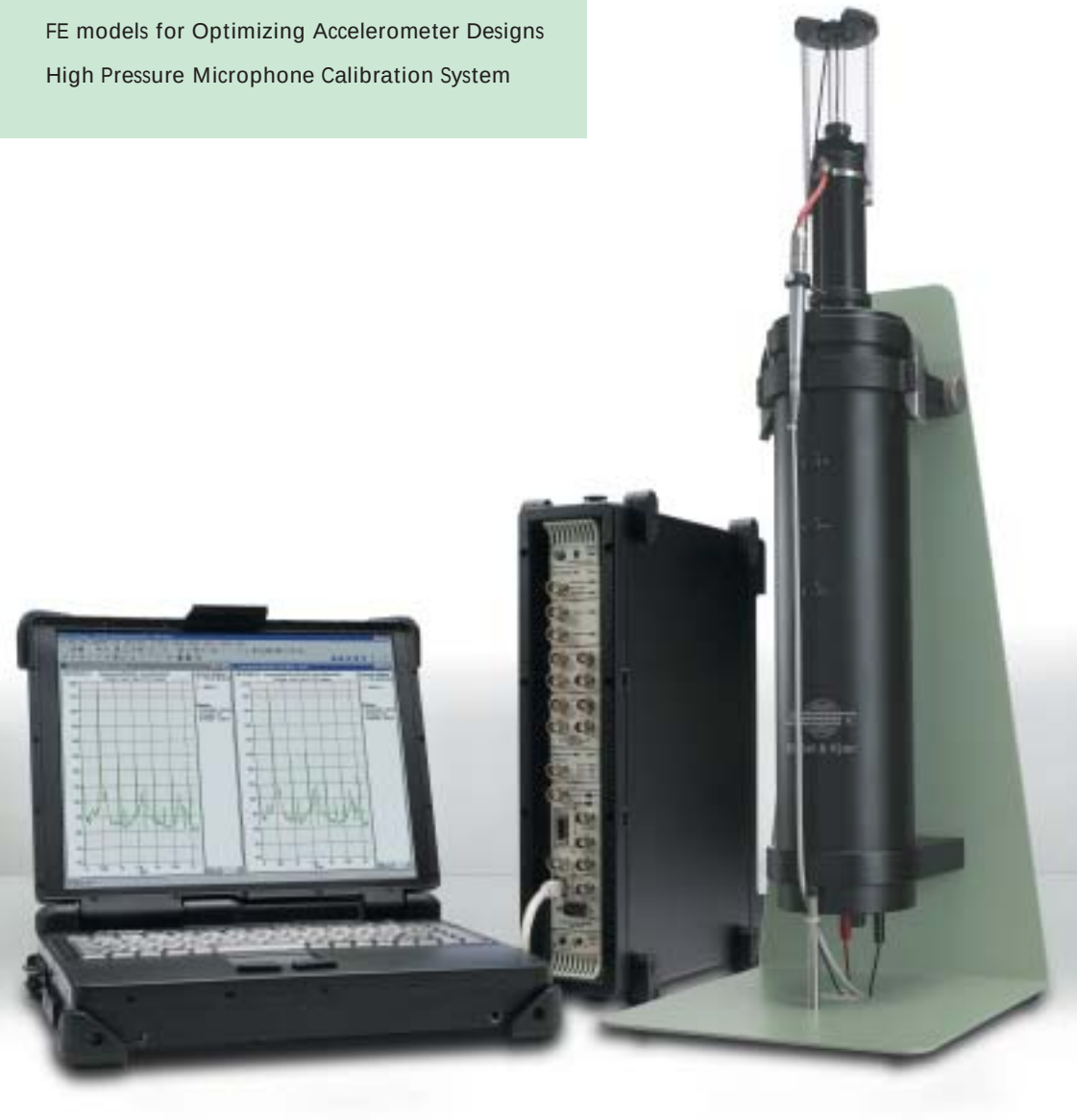

No.1 2002

Brüel & Kjær

Previously issued numbers of Brüel & Kjær Technical Review

1 – 2001 The Influence of Environmental Conditions on the Pressure Sensitivity of Measurement Microphones
Reduction of Heat Conduction Error in Microphone Pressure Reciprocity Calibration
Frequency Response for Measurement Microphones – a Question of Confidence
Measurement of Microphone Random-incidence and Pressure-field Responses and Determination of their Uncertainties

1 – 2000 Non-stationary STSF

1 – 1999 Characteristics of the vold-Kalman Order Tracking Filter

1 – 1998 Danish Primary Laboratory of Acoustics (DPLA) as Part of the National Metrology Organisation
Pressure Reciprocity Calibration – Instrumentation, Results and Uncertainty
MP.EXE, a Calculation Program for Pressure Reciprocity Calibration of Microphones

1 – 1997 A New Design Principle for Triaxial Piezoelectric Accelerometers
A Simple QC Test for Knock Sensors
Torsional Operational Deflection Shapes (TODS) Measurements

2 – 1996 Non-stationary Signal Analysis using Wavelet Transform, Short-time Fourier Transform and Wigner-Ville Distribution

1 – 1996 Calibration Uncertainties & Distortion of Microphones.
Wide Band Intensity Probe. Accelerometer Mounted Resonance Test

2 – 1995 Order Tracking Analysis

1 – 1995 Use of Spatial Transformation of Sound Fields (STSF) Techniques in the Automative Industry

2 – 1994 The use of Impulse Response Function for Modal Parameter Estimation
Complex Modulus and Damping Measurements using Resonant and Non-resonant Methods (Damping Part II)

1 – 1994 Digital Filter Techniques vs. FFT Techniques for Damping Measurements (Damping Part I)

2 – 1990 Optical Filters and their Use with the Type 1302 & Type 1306 Photoacoustic Gas Monitors

1 – 1990 The Brüel & Kjær Photoacoustic Transducer System and its Physical Properties

2 – 1989 STSF — Practical Instrumentation and Application
Digital Filter Analysis: Real-time and Non Real-time Performance

1 – 1989 STSF — A Unique Technique for Scan Based Near-Field Acoustic Holography Without Restrictions on Coherence

2 – 1988 Quantifying Draught Risk

(Continued on cover page 3)

Technical Review

No. 1 – 2002

Contents

Editor: Harry K. Zaveri

A New Design Principle for Triaxial, Piezoelectric Accelerometers*

Knud Styhr Hansen

Abstract

In a previous paper (SENSOR 1997), the principle of a triaxial, piezoelectric accelerometer was described. This has relatively few parts compared to traditional, triaxial accelerometers which normally contain three single, axial units and are mounted in a common housing with their axes perpendicular to each other. The design was built around one piezoelectric ring suspended on four simple supports and carrying a seismic mass in the centre. The signals were taken as charge signals from two of the supports and as a voltage signal from the central mass.

This paper describes a similar design but with the piezoelectric ring suspended on only three simple supports. Here, the signals can be taken as charge signals from each of the three supports with the central mass grounded. Special signal conditioning (built into the accelerometer) is needed to make the output signals represent the three axes of a Cartesian system of coordinates. Compared with the four-support design, this design has greatly improved performance regarding environmental parameters such as base-strain sensitivity and temperature-transient sensitivity. The basic theory behind the principle is explained and measurement results from a very compact, practical unit are also described.

Résumé

Un précédent article (SENSOR 1997) avait décrit le principe de fonctionnement d'un accéléromètre piézoélectrique triaxial composé de moins d'éléments que les accéléromètres triaxiaux conventionnels, qui comportent généralement trois parties, une pour chaque axe, réciproquement orthogonales dans un boîtier unique. Ce modèle consistait en une bague piézoélec-

* First printed at the 8th International Congress on Sound and Vibration, Hong Kong, 2001.

trique entourant une masse sismique et simplement suspendue par quatre supports. Les signaux de charge passaient par deux des supports et le signal de tension par la masse centrale.

Cet article est la description d'une construction similaire, mais où l'élément piézoélectrique est maintenant suspendu à trois supports au lieu de quatre. Les signaux fournis sont des signaux de charge provenant de chacun des trois supports, la partie centrale étant reliée à la masse électrique. Un conditionneur spécial, intégré à l'accéléromètre, est requis pour que les signaux de sortie puissent représenter les trois axes d'un système de coordonnées cartésien. Comparé au modèle précédent à quatre supports, cette conception résulte en une amélioration très significative des performances au regard des paramètre environnementaux (sensibilité aux contraintes sur la base et aux fluctuations de température. Le principe de fonctionnement est ici expliqué, et les résultats obtenus avec ce petit instrument pratique et très compact sont également publiés.

Zusammenfassung

In einem früheren Artikel (SENSOR 1997) wurde das Prinzip eines piezoelektrischen Triaxial-Beschleunigungsaufnehmers beschrieben. Dieser besteht aus relativ wenigen Teilen – verglichen mit traditionellen triaxialen Aufnehmern, die in der Regel aus drei Aufnehmern bestehen, die mit senkrecht aufeinander stehenden Achsen in einem gemeinsamen Gehäuse untergebracht sind. Bei der beschriebenen Bauart war eine seismische Masse von einem piezoelektrischen Ring umgeben, der auf vier Stützen ruhte. Die Signale wurden als Ladungssignale von zwei der Stützen und als Spannungssignal von der Zentralmasse abgenommen.

Dieser Artikel beschreibt eine ähnliche Bauart, wobei der piezoelektrische Ring jedoch nur auf drei Stützen ruht. Hier können Ladungssignale von jeder der drei Stützen abgenommen werden, während die Zentralmasse geerdet ist. Es ist eine besondere Signalkonditionierung erforderlich (im Aufnehmer integriert), damit die Ausgangssignale die drei Achsen eines kartesischen Koordinatensystems repräsentieren. Verglichen mit der älteren Bauart mit vier Stützen ist das Verhalten hinsichtlich Umgebungsparametern wie Basisdehn- und Temperatursprungempfindlichkeit wesentlich verbessert. Der Artikel erläutert die Grundtheorie hinter dem Prinzip und beschreibt auch Messergebnisse mit diesem sehr kompakten, praktischen Aufnehmer.

Introduction

It is a general wish to produce even smaller and lighter accelerometers which can measure vibrations on yet lighter structures without affecting the vibration pattern of the measuring object. However, making a seismic accelerometer lighter also means making it less sensitive and this limits the effective dynamic range of the transducer. In particular for triaxial measurements, weight can be a problem as you have the weight of three units loading the same mounting point.

This paper describes a triaxial piezoelectric accelerometer in which the three axes share a common PZ-ring and seismic mass. This considerably reduces the weight/sensitivity ratio compared with the usual design of three individual units in a common housing. At the same time, the accelerometer shows strongly improved specifications regarding base-bending sensitivity compared to previous 'common PZ-ring and mass' accelerometers.

Calculation of Reaction Forces in the Supports

Fig. 1 shows a solid cylindrical body suspended on three simple supports (hinges) separated by 120° along the periphery of one end of the cylinder. A force, *F*, is applied at the centre of gravity at an angle, α, in relation to the X-axis. The projection of the force, *F*, on the YZ-plane makes an angle, β, in relation to the Z-axis. F_A, F_B and F_C are the reaction forces in the supports in the X-direction.

At frequencies well below the first resonance frequency of the system, the static equilibrium equations can be used for calculation of the forces in the supports.

The force, *F*, is divided into three components: $F_x = F\cos\alpha$ (parallel to the X-axis), $F_y = F\sin\alpha\sin\beta$ (parallel to the Y-axis), and $F_z = F\sin\alpha\cos\beta$ (parallel to the Z-axis). For the sake of simplicity, the calculations are made for the three components separately and the results summed afterwards.

For the force component in the Y-direction, $F_y = F\sin\alpha\sin\beta$

The sum of forces of reaction in the X-direction must equal zero, as F_Y has no component in the X-direction:

$$F_{AY} + F_{BY} + F_{CY} = 0$$

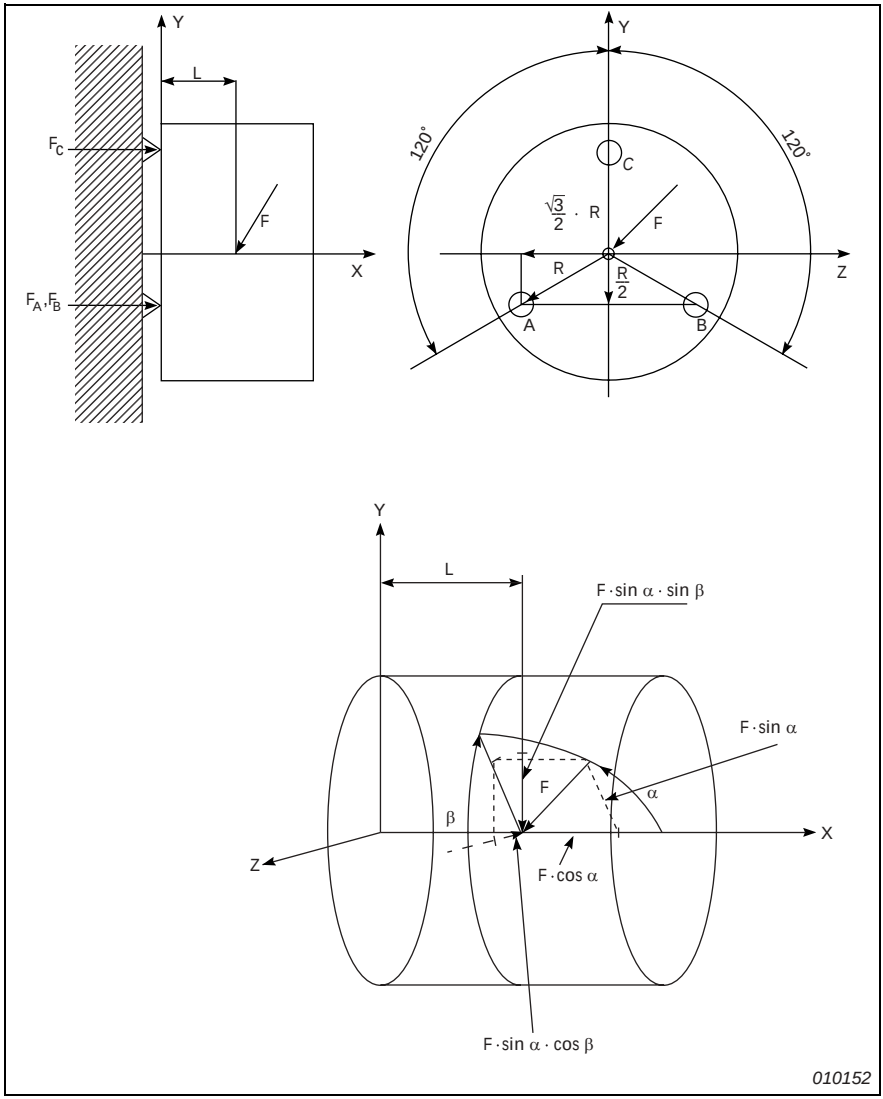

Fig. 1. Forces acting on a cylindrical body

The sum of the bending moments around the Z-axis of all the forces equals zero:

$$-F_{AY}\frac{R}{2} - F_{BY}\frac{R}{2} + F_{CY}R + F_Y L = 0$$

where R is the distance between the centre and the supports, and L is the distance between the YZ-plane and the attack point of the force.
The sum of the bending moments around the Y-axis of all the forces equals zero:

$$F_{AY}\frac{\sqrt{3}}{2}R - F_{BY}\frac{\sqrt{3}}{2}R = 0$$

From these equations, F_{AY}, F_{BY} and F_{CY} can be found:

$$F_{AY} = F_{BY} = \frac{1}{3}\frac{F_Y L}{R}$$

$$F_{CY} = \frac{-2}{3}\frac{F_Y L}{R}$$

For the force component in the Z-direction, $F_Z = F\sin\alpha\cos\beta$
The sum of forces of reaction in the X-direction must equal zero as F_Z has no component in the X-direction:

$$F_{AZ} + F_{BZ} + F_{CZ} = 0$$

The sum of the bending moments around the Z-axis of all the forces equals zero:

$$-F_{AZ}\frac{R}{2} - F_{BZ}\frac{R}{2} + F_{CZ}R = 0$$

The sum of the bending moments around the Y-axis of all the forces equals zero:

$$-F_{AZ}\frac{\sqrt{3}}{2}R + F_{BZ}\frac{\sqrt{3}}{2}R + F_Z L = 0$$

From these equations, F_{AZ}, F_{BZ} and F_{CZ} can be found:

$$F_{AZ} = \frac{1}{\sqrt{3}}\frac{F_Z L}{R}$$

$$F_{BZ} = \left(-\frac{1}{\sqrt{3}}\right)\frac{F_Z L}{R}$$

$$F_{CZ} = 0$$

For the force component in the X-direction, $F_X = F\cos\alpha$

As F_X is an axial, central force, this gives no bending moment so the reaction forces must be equally distributed on the three supports:

$$F_{AX} = F_{BX} = F_{CX} = \frac{1}{3}F_X$$

For the combined force F

By addition of the three components, the total reaction forces in the X-direction of the three supports are found:

$$F_A = F_{AY} + F_{AZ} + F_{AX} = \frac{FL}{3R}\sin\alpha(\sin\beta + \sqrt{3}\cos\beta) + \frac{1}{3}F\cos\alpha$$

$$F_B = F_{BY} + F_{BZ} + F_{BX} = \frac{FL}{3R}\sin\alpha(\sin\beta - \sqrt{3}\cos\beta) + \frac{1}{3}F\cos\alpha$$

$$F_C = F_{CY} + F_{CZ} + F_{CX} = \frac{-2}{3}\frac{FL}{R}\sin\alpha\sin\beta + \frac{1}{3}F\cos\alpha$$

Calculation of Charges on PZ-ring

Fig. 2 shows an arrangement in which the solid cylinder from Fig. 1 is replaced by a piezoelectric ring with a mass in the centre and surrounded by three arms, each of which is curved as part of a cylinder. In this case, a shear force will occur in each of the sectors of the piezoelectric ring corresponding to the reaction forces F_A, F_B and F_C.

If the piezoelectric ring is polarised in the axial direction, the shear force will cause an electric charge on each sector of the PZ-ring, which is equal to d_{15} times the reaction force:

$$Q_A = d_{15}\frac{FL}{3R}\sin\alpha(\sin\beta + \sqrt{3}\cos\beta) + d_{15}\frac{1}{3}F\cos\alpha$$

$$Q_B = d_{15}\frac{FL}{3R}\sin\alpha(\sin\beta - \sqrt{3}\cos\beta) + d_{15}\frac{1}{3}F\cos\alpha$$

$$Q_C = (-2)d_{15}\frac{FL}{3R}\sin\alpha\sin\beta + d_{15}\frac{1}{3}F\cos\alpha$$

where d_{15} is the piezoelectric constant for shear action.

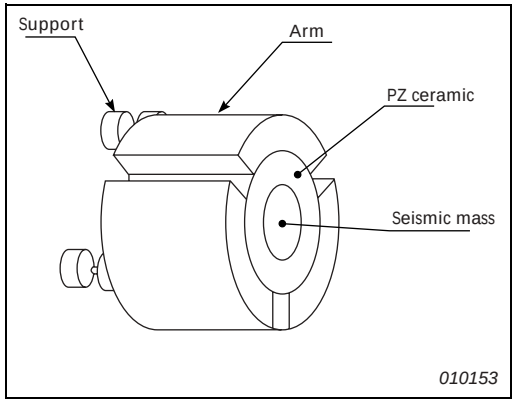

Fig. 2. Schematic drawing of centre unit

By suitably adding and subtracting the various expressions, it is possible to obtain signals which represent the three axes of a Cartesian system of coordinates:

$$Q_X = Q_A + Q_B + Q_C = d_{15} F \cos\alpha$$

$$Q_Y = Q_A + Q_B - 2Q_C = 2d_{15}\frac{FL}{R}\sin\alpha\sin\beta$$

$$Q_Z = Q_A - Q_B = \frac{2}{\sqrt{3}}d_{15}\frac{FL}{R}\sin\alpha\cos\beta$$

As can be seen, Q_X , Q_Y and Q_Z represent the three orthogonal axes of a system of coordinates. Q_X has its maximum for $\alpha = 0$, which means that it represents the axial direction. Q_Y and Q_Z have their maxima in the YZ-plane ($\alpha = 90°$) with a mutual angular spacing of 90° which appears from the sine and cosine functions of β, respectively.

The described system constitutes an accelerometer. If it is vibrated with an acceleration, a, the force, F , will be the inertial force from the seismic mass:

$$F = Ma$$

The sensitivity in the three axis-directions will then be:

$$\frac{Q_X}{a_X} = d_{15} M_c$$

$$\frac{Q_Y}{a_Y} = 2d_{15}\frac{ML}{R}$$

$$\frac{Q_Z}{a_Z} = \frac{2}{\sqrt{3}}d_{15}\frac{ML}{R}$$

It must be noted that M_c, in the expression of the X-axis sensitivity, is only the central mass plus approximately half of the mass of the piezoelectric ring. In the expressions of the Y- and Z-axes sensitivities, M is the total mass of the system including central mass, piezoelectric ring and the arms.

Electrical Circuit

It may seem to be a bit complicated that one has to add and subtract different expressions before the signals emerge as X-, Y-, and Z-signals. However, it can be done fairly easy as one can see from the schematics in Fig. 3.
The charge signal for the X-axis ($Q_A + Q_B + Q_C$) is available at the central mass. Relative to the central mass, points *A*, *B*, and *C* (in Fig. 3) can be assumed to be grounded as they are connected to the input of charge amplifiers. This means that the signal from the central mass can go directly to the X-charge amplifier, the output of which will be:

$$\frac{1}{C_X}(Q_A + Q_B + Q_C)$$

The value ($Q_A - Q_B$) is also fairly easy to generate. Q_A is simply inverted in a charge converter and the result added to Q_B in the Z-charge amplifier. The output from this will be:

$$\frac{1}{C_Z}(Q_A - Q_B)$$

The Y-output, $Q_Y = (Q_A + Q_B - 2Q_C)$, is obviously the most complicated signal to obtain. However, from the X-output, it is fairly easy to generate a charge of one third of the charge from the central mass. By adding this to Q_C, the output from the Y-charge amplifier will be:

$$\frac{1}{3C_Y}(Q_A + Q_B - 2Q_C)$$

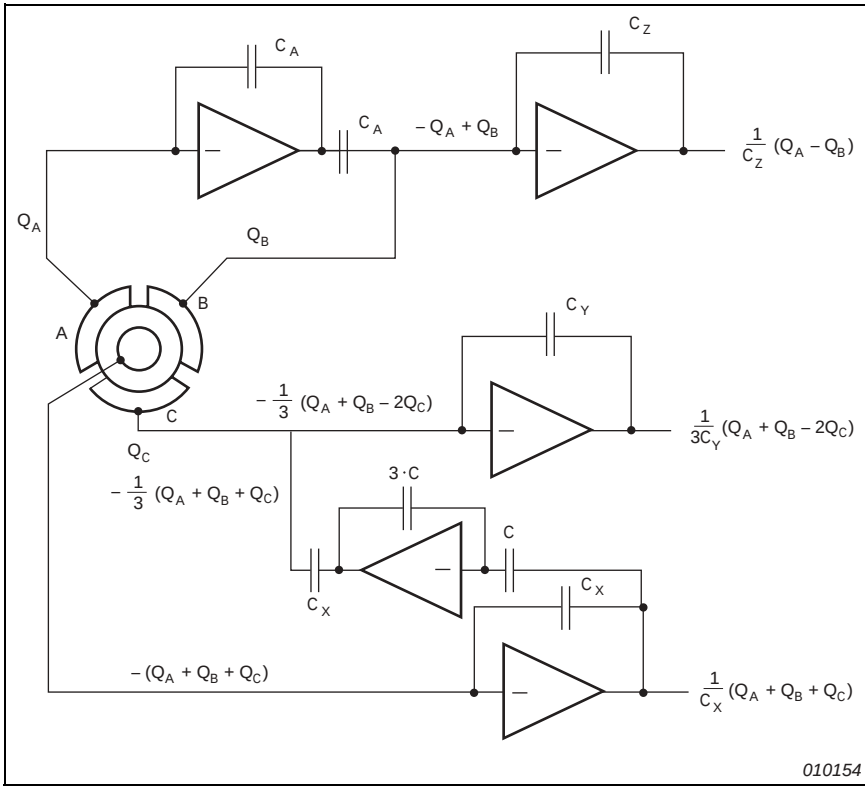

Fig. 3. Block diagram of electrical circuit

Practical Solution

Fig. 4 shows a cross-section of an accelerometer built according to the described principle. As seen, the three supports (hinges) are mounted on a ceramic substrate which, at the same time, constitutes the hybrid circuit with the amplifiers. The supports also establish the electrical connections between the piezoelectric ring and the substrate. As the cable connector also goes directly into the hybrid, the whole system requires just one lead wire between the central mass and the hybrid, which highly simplifies the assembly.

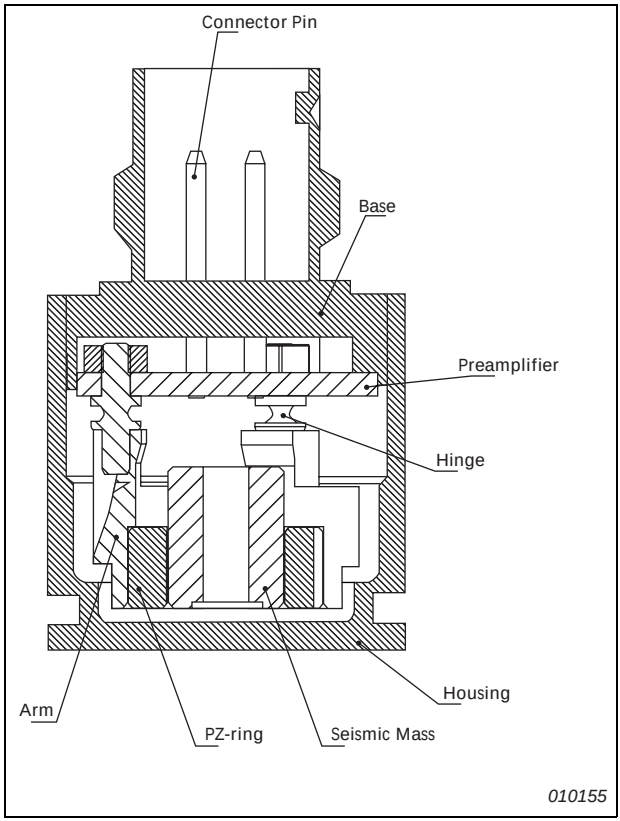

Fig. 4. Sectional view of the accelerometer

The mechanical and piezoelectric specifications of the system, referred to in the terminology used in this paper, are as follows:

R = 3.10 mm
L = 3.62 mm
M_c = 0.607 gram
M = 1.91 gram
d_{15} = 540 pC/N

From these specifications, the sensitivities can be calculated. The results are shown below with the measured values in parentheses.

$$\frac{Q_X}{a_X} = d_{15} M_c = 0.327\,\text{pC/ms}^{-2};\ (\text{measured: } 0.328\,\text{pC/ms}^{-2})$$

$$\frac{Q_Y}{a_Y} = 2 d_{15} \frac{ML}{R} = 2.41\,\text{pC/ms}^{-2};\ (\text{measured: } 2.38\,\text{pC/ms}^{-2})$$

$$\frac{Q_Z}{a_Z} = \frac{2}{\sqrt{3}} d_{15} \frac{ML}{R} = 1.39\,\text{pC/ms}^{-2};\ (\text{measured: } 1.38\,\text{pC/ms}^{-2})$$

As seen, the agreement between calculated and measured values is very close. The sensitivity varies in different directions, but this can be adjusted by the correct choice of the feedback capacitors C_X, C_Y, and C_Z.

Achieved Specifications

The following main specifications were achieved:

- Sensitivity: 10 mV/ms^{-2}
- Mounted resonance Y and Z: 9.8 kHz; X: 22 kHz
- Dynamic Range, broad band 108 dB (200 µg to 50 g)
- Weight: 4.8 gram
- Dimensions: 10 × 10 × 10 mm
- Cross Axis Sensitivity: < 5 %
- Base Strain Sensitivity: 0.0006 ms^{-2}/µε

Concluding Remarks

Compared with the ordinary way of designing a triaxial accelerometer, the new design has many advantages.

As the three directions share a common mass, the sensitivity can be higher for the same total weight and size. It also means much fewer mechanical parts. For example, a Brüel&Kjær DeltaShear® triaxial accelerometer has 9 seismic masses and 9 flat PZ elements while the new design has one seismic mass and one PZ-ring.

Also, the fact that the whole accelerometer can be built on the connector/ base assembly and inserted into the housing from one side, leaving the other five sides usable for mounting slots or threads, makes the design more versatile.

Compared with its 'four-suspended' predecessor, the base-strain sensitivity is reduced dramatically from 0.03 $ms^{-2}/\mu\varepsilon$ for the old design to 0.0006 $ms^{-2}/\mu\varepsilon$ for the new design. The reason for this is that the new design has three hinges instead of four. It is not possible to transfer a bending moment from the base to the PZ-ring through three simple supports.

References

[1] J. Tichý and G. Gautschi, *"Piezoelectrische Messtechnik"*

[2] Knud Styhr Hansen, *"A New Design Principle for Triaxial Piezoelectric Accelerometers"*, SENSOR 1997

Use of FE Models in the Optimisation of Accelerometer Designs

By B. Liu & B. Kriegbaum

Abstract

This paper describes the design process of a recently introduced Annular Shear Piezoelectric Accelerometer Type 4511. The accelerometer, which is piezoceramic, has an insulated and double-shielded housing made of stainless steel (AISI 316 L), while the seismic mass is made of tungsten. All processes and materials comply with standard MIL–STD–11268. The mounted resonance frequency exceeds 40 kHz, and the sensitivity is 10 mV/g ±5 %. During development, the new design is evaluated and optimised using a Finite Element (FE) simulation before making the actual prototype. Reasonable agreement between the experimental results of the physical prototype and the simulation results is achieved. This use of the FE model facilitates the design process in the optimisation of the accelerometer. In addition, Type 4511 has a built-in DeltaTron® charge amplifier with ID and complies with the IEEE–P 1451.4 standard which is a smart transducer interface for sensors including mixed-mode communication protocols and transducer electronic data sheet (TEDS).

Résumé

Le présent article décrit le processus de conception d'un Accéléromètre piézoélectrique à cisaillement annulaire, récemment introduit sur le marché, le Type 4511. Son boîtier en acier inoxydable AISI 316 L est isolé et à double blindage. Un matériau en Piézocéramique PZ 23 est utilisé. La masse sismique est en tungsten. Tous les procédés et matériaux sont conformes à MIL – STD-11268. La fréquence de résonance de l'ensemble monté dépasse 40 kHz. La sensibilité est de 10 mV/g ±5 %. Cette nouvelle construction a d'abord été virtuellement évaluée et optimisée par simulation (éléments finis), avant le prototypage proprement dit. Une bonne concordance a été obtenue entre les résultats d'essais effectués sur le prototype et les calculs de simulation. Cette méthode optimise l'efficacité des concepteurs. En outre, le 4511 est équipé d'un amplificateur de charge DeltaTron® intégré avec sa fiche électronique TEDS, conformément à IEEE – P1451.4. Cette interface

intelligente de communication inclut, outre les données d'identification et les caratéristiques des capteurs, les protocoles de communication en mode mixte.

Zusammenfassung

Dieser Artikel beschreibt den Konstruktionsprozeß eines neuen piezoelektrischen Ring-Shear-Beschleunigungsaufnehmers, Typ 4511. Diese Bauart besitzt ein isoliertes und doppelt abgeschirmtes Gehäuse. Das Aufnehmergehäuse besteht aus rostfreiem Stahl, AISI 316 L. Es wird piezokeramisches Material PZ 23 verwendet. Die seismische Masse besteht aus Wolfram. Alle Prozesse und Werkstoffe entsprechen MIL – STD – 11268. Die Resonanzfrequenz des montierten Aufnehmers überschreitet 40 kHz. Der Übertragungsfaktor beträgt 10 mV/g ±5%. In der Konstruk-tionsphase wird die neue Bauart bewertet und mit Hilfe von Finite-Elemente (FE)-Simulation optimiert, bevor der eigentliche Prototyp gefertigt wird. Es wird eine zufriedenstellende Übereinstimmung zwischen den experimentellen Ergebnissen am physikalischen Prototyp und den Simulationsergebnissen erreicht. Damit wird die Bauart effizienter. Darüber hinaus besitzt Typ 4511 einen integrierten DeltaTron® Ladungsverstärker mit ID und erfüllt die Norm IEEE P 1451.4, d.h. er besitzt eine intelligente Sensorschnittelle mit „Mixed-mode" Kommunikationsprotokollen und TEDS (Transducer Electronic Data Sheet).

Introduction

Piezoelectric accelerometers are widely used for vibration measurements. Generally speaking, they have been modelled using analytical and combined analytical-experimental methods. The analytical method uses an electrical circuit model developed on the basis of the electromechanical analogy. After theoretical analysis of the design is made, a prototype is manufactured. Almost always, the prototype does not have the characteristics of the theoretical model and modifications have to be carried out several times. This is a time-consuming and costly affair.

With the advent of inexpensive and fast computers, numerical techniques have rapidly evolved to solve physical problems in contemporary engineering analysis and design – the FE method is one such technique. It can be flexibly used to model any arbitrary geometry and characterise any given material property. This numerical technique has been used as a new development tool for the design of piezoelectric accelerometers by Brüel & Kjær.

In this paper, the design of the new Annular Shear Accelerometer Type 4511, which has special requirements, is described. The Type 4511 accelerometer is designed for installation in a helicopter transmission's main gearbox, as well as its intermediate and tail gearboxes, for continuous monitoring of the gearbox housing's vibration. The accelerometer's signal output is a voltage proportional to the instantaneous acceleration, while the sensitivity is 10 mV/g ±5%. Mounted resonance frequency should exceed 40 kHz when measured with the accelerometer properly installed. In addition to these requirements, the new accelerometer should have a built-in DeltaTron® charge amplifier with ID and comply with the IEEE–1451.4 standard.

Design and Modelling

Because the accelerometer is meant to be mounted permanently on board a helicopter, its primary characteristic is absolute robustness. Secondly, it is designed so as not to be sensitive to electromagnetic interference (EMI) signals, while having a side connector which can be mounted in any direction. After considering the variety of designs available at Brüel&Kjær, the Annular Shear design was chosen as being most suitable.

Normally, in Annular Shear design, the piezoelectric element and the mass are rings which are mounted around a centre post, with all elements being held in position using mechanical pre-loading. In this case, rather than using a clamping ring which is a costlier process, the three elements are soldered together with tin. PZ23 piezoceramic is used for the sensing part, while the seismic mass is made of tungsten and the housing of stainless steel (AISI316L).

Fig. 1 shows a schematic drawing of the Annular Shear accelerometer comprising a ceramic element of mass, m, which is fixed between the centre post and the freely supported seismic mass, M. This structure can provide low sensitivity to base-bending, temperature-transients, high sound-pressure levels, etc., and can work in any direction.

The new accelerometer differs from former Brüel&Kjær Annular Shear accelerometers in that it has a centre bolt. This bolt makes the positioning of the side connector possible in any direction.

As mentioned previously, the accelerometer should be protected from the influence of high- and/or low-frequency EMI signals. Therefore, it has an insulated and double-shielded housing which breaks the ground loop. It also prevents radiated EMI from disturbing the vibration signal.

In this design, the housing of the accelerometer is treated as the outside case to act as a shield against high frequencies (>100 kHz), usually radio frequencies.

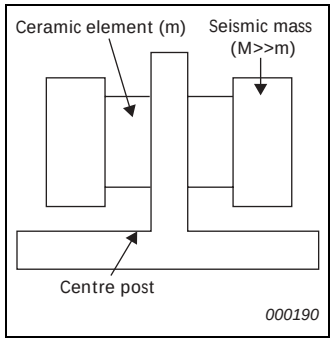

Fig. 1. Schematic drawing of the Annular Shear Accelerometer

The inner case is made from brass, shown later to shield the accelerometer from low frequencies, such as 50 or 400 Hz electrical mains frequency.

In order to make the design more efficient and get more understanding of the accelerometer operation, FE simulation has been used during the design process.

The structure and the ceramic material are modelled with element SOLID45 and element SOLID5, respectively, as defined in ANSYS® [2]. The piezoelectric material is poled in the upward direction in the axial direction. Its properties are given in Table 1 [4]. The structure is modelled as 3D, solid material. Table 2 shows the properties used in the model for these materials. The charge sensitivity is calculated at 159.2 Hz using ANSYS® Harmonic Analysis by applying force to the mounted surface of the computer model. The mounted resonance frequency is calculated by using ANSYS® Modal Analysis by assuming the accelerometer is mounted on an infinitely rigid and heavy body.

Density (kg/m^3)	7700	
Relative Dielectric Constants	e^S_{11}/e_0	830
	e^S_{22}/e_0	830
	e^S_{33}/e_0	916
Elastic Compliance (10^{-12} m^2/N)	S^E_{11}	15
	S^E_{12}	-5.74
	S^E_{13}	-7.22
	S^E_{33}	19
	S^E_{44}	47.5
	S^E_{66}	44.3
Piezoelectric Charge Coefficients (10^{-12} C/N)	d_{31}	-130
	d_{33}	330
	d_{15}	335

Table 1. Piezoelectric material properties

Material	Density (kg/m^3)	Young's modulus (10^{10} N/m^2)	Poisson's ratio
Tungsten alloy	17500	34	0.27
Stainless steel	7860	20	0.30
Aluminum	2700	7.1	0.32
Brass	8600	10.4	0.37

Table 2. Material properties for the structures

During the design process, three major versions were made as shown in Fig. 2. The pink colour denotes the housing made of stainless steel while red denotes the seismic mass made of tungsten alloy. Cyan denotes the piezoelectric material made of PZ23. The purple denotes the hybrid circuit that is the preamplifier. In the computer models, the preamplifier is treated only as a mechanical part. Orange denotes the inner case made of brass and blue denotes the centre

post. The model shown in Fig. 2(a) has an aluminum centre post while that in (b) is of stainless-steel and (c) tungsten alloy.

Comparison of the three models' specifications is given in Table 3.

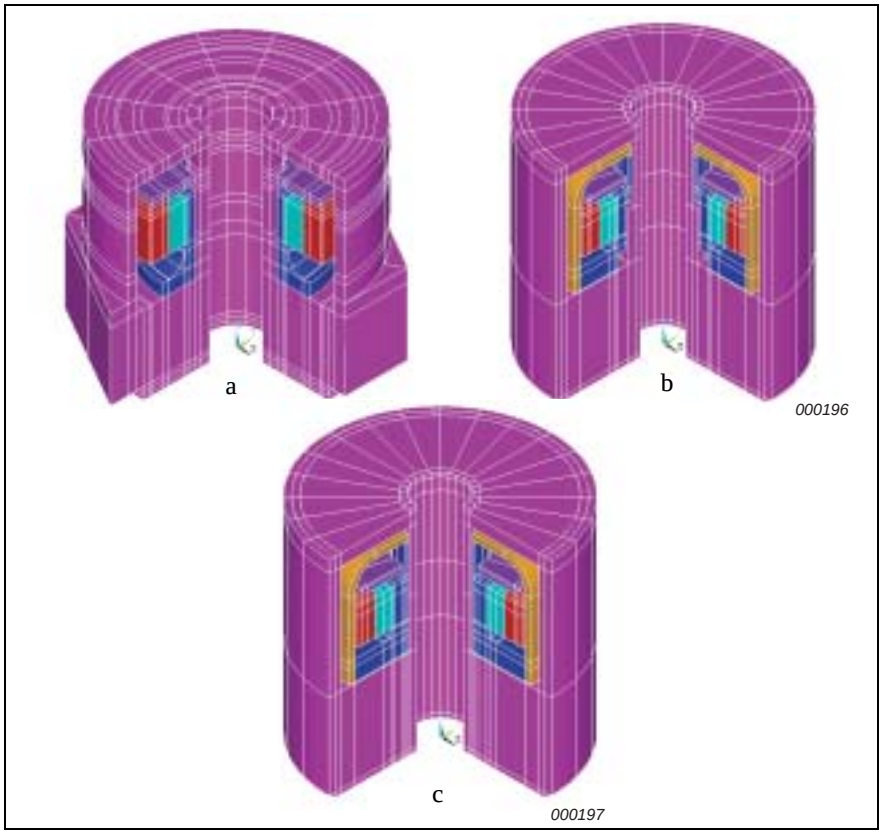

Fig. 2. The accelerometer structures

The results in the first three rows are obtained by neglecting the centre bolt which means that the model is mounted on an infinitely rigid body by surface to-surface contact. The results in the fourth row are obtained by mounting the model with a centre bolt but with the pre-stress neglected.

	Mounted Resonance Frequency (Hz)	Transverse Resonance Frequency (Hz)	Charge Sensitivity (10^{-12} C/ms^{-2})
Version 1(a)	49544	23315	1.56
Version 2(b)	51742	20299	0.83
Version 3(c)	43368	25240	1.45
Version 3(c)'	43815	24816	1.45

Table 3. Comparison of the three models' specifications

Version 1 does not have an inner case to shield the accelerometer from low frequencies. Therefore, though the specifications can fulfill the requirements, it has to be improved to Version 2 that has an inner case. From Fig. 2(b), it can be seen that the centre post has a very complicated structure instead of being straight. It is because the wall of the housing had to be thick in order to make sure it was strong enough for mounting the accelerometer with a centre bolt. Obviously, it would make manufacturing difficult. Further studies showed that a straight wall could also withstand the pre-load from the centre post which resulted in Version 3. The centre post in version 3(c) is glued to the base which breaks the ground loop.

Based on the understanding of Annular Shear design, both the shear-force distribution and the voltage distribution of the ceramic should be the same along the longitudinal axis at any radius. Fig. 3(a) and (b) show the shear force and the voltage distribution of the ceramic shown in Fig. 2(c), respectively. The discrepancy for the shear stress is due to the effects of boundary conditions.

Mounted resonance frequency is a rather important specification of accelerometers and is difficult to estimate analytically. Using a computer model, however, the resonance frequencies, as well as the mode shapes can be displayed. Fig. 5 shows three resonance modes. The direction and colour of the arrows represent the direction and the amplitude of the displacement of each component. In Fig. 5, (c) is the vertical mode which is the main mode at 43368 Hz. (a) is the transverse mode at 25240 Hz, and (b) the torsional mode at 35379 Hz. In fact, the main mode is the 8^{th} mode, which means there are a lot of resonance frequencies in the lower frequency range. It is very important to make sure that these modes, such as the torsional mode, should not yield a large output to reduce the usable frequency range. Fig. 4 is the charge sensitivity plot. It can be seen that the curve is very smooth, with no undesirable peaks, indicating a very

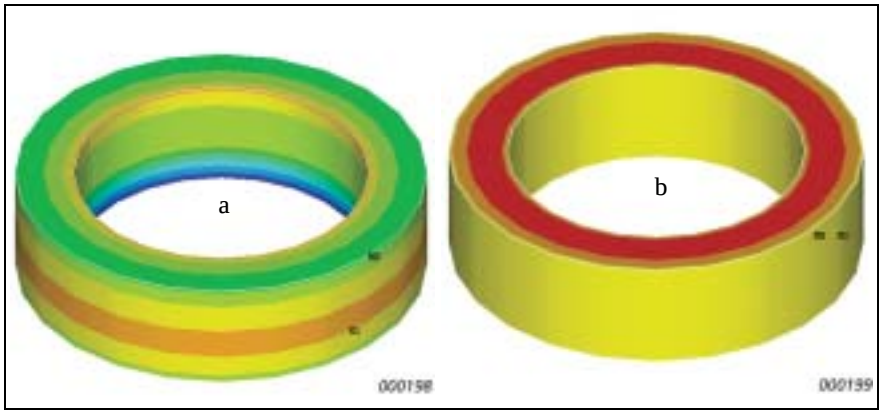

Fig. 3. Shear stress and Voltage distribution of the ceramic ring

wide, usable frequency range. Once the design was sufficiently optimised using computer simulation, a prototype was made according to Fig. 2(c).

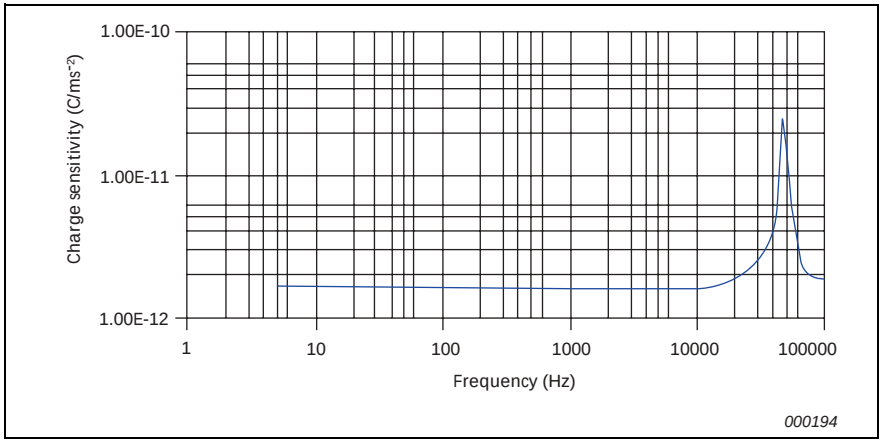

Fig. 4. Charge sensitivity plot

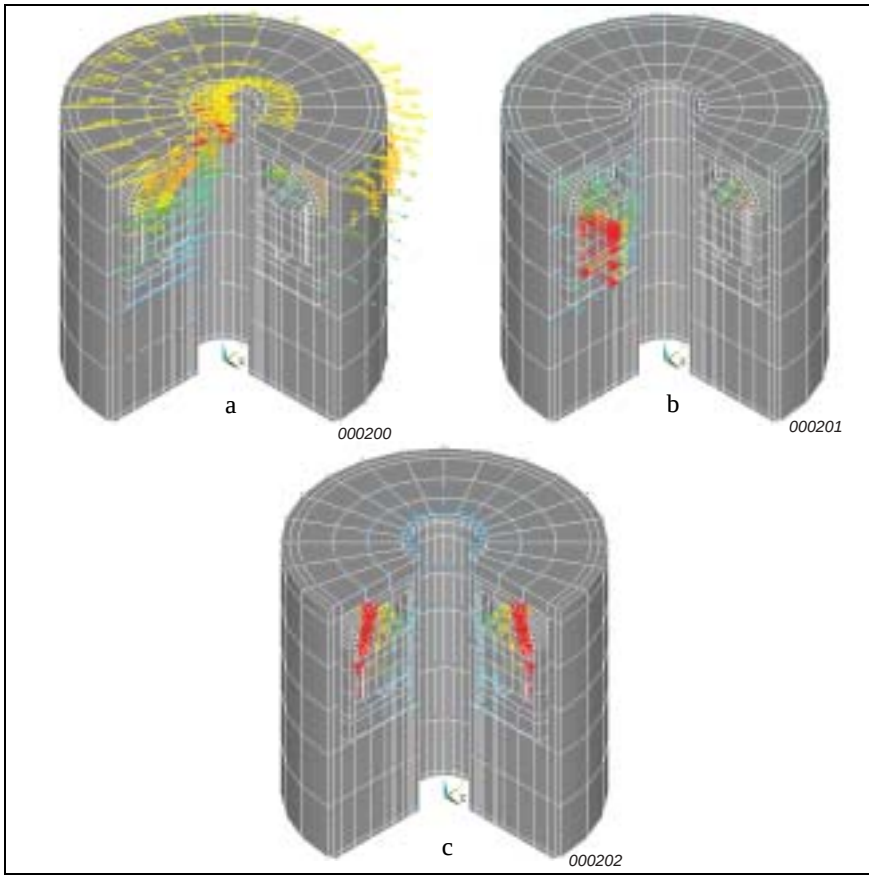

Fig. 5. Resonance modes: (a) Transverse mode 25240 Hz; (b) Torsional mode 35379 Hz; (c) Vertical mode 43368 Hz

Experimental Verification

The sensitivity of the accelerometer prototype is measured using Brüel&Kjær Calibration System 9610. Fig. 6 shows the set-up that is used for measurement of the frequency response.

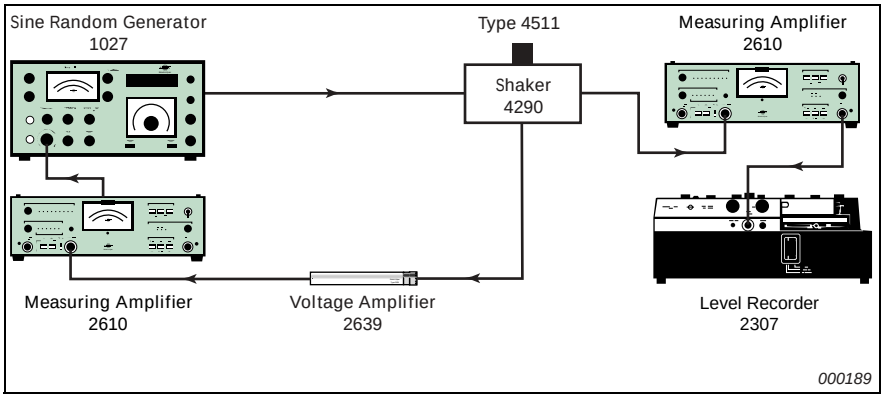

Fig. 6. A setup for measuring the frequency response of Type 4511

The FE simulation and experimental results are compared in Table 4. As the use of the centre bolt has very little influence, the data shown in the table were obtained without using it.

Specification	FE simulation results	Experimental results	Deviation
Charge sensitivity (pC/ms^{-2})	1.45	1.4	3.57%
Mounted resonance frequency (kHz)	43.4	41	5.86%

Table 4. Comparison between simulation and experimental results

From Table 4, it can be seen that the measured sensitivity of the prototype is a charge sensitivity of 1.4 pC/ms^{-2} instead of the target voltage-sensitivity of 10 mV/g. To achieve this, an appropriate capacitor is chosen in the feedback of the charge convertor.

Table 4 shows that there are no significant discrepancies between the FE simulation and measured results. The deviation between the FE simulation and the measured sensitivity is 3.57%, while the deviation of the mounted resonance frequency is 5.86%.

The results thus show very clearly that the computer model can be used efficiently to guide the design.

DeltaTron® Charge Amplifier With ID

Type 4511 has a built-in DeltaTron® charge amplifier with ID and complies with IEEE–1451.4 standard, which is a smart transducer interface for sensors including mixed-mode communication protocols and transducer electronic data sheet (TEDS).

IEEE–1451 Working Groups have been working on a uniform approach for connecting sensors to communication networks, control systems and measurement systems, [3]. The 1451.1, 1451.2 and 1451.3 efforts focus on network-capable sensors with digital readings. The 1451.4 effort proposes a mixed-mode smart transducer communication protocol based on existing analog connections.

The key considerations for TEDS design are: relevant information that helps the user, plug-and-play functionality, support for all transducers and openness for individual needs. The 1451.4 TEDS includes Identification Parameters, Device Parameters, Calibration Parameters and Application Parameters.

The benefits of the ID (TEDS) are:

- No mistakes in data entry due to download of transducer sensitivity from accelerometer
- Transducer swaps on the fly without having to make setup changes
- Possibility for corrections of amplitude and/or phase response using stored in TEDS

Results and Summary

A new Annular Shear piezoelectric accelerometer Type 4511, which has a built-in DeltaTron® charge amplifier with ID and complies with IEEE–1451.4 standard, has been designed using PZ23 as sensing part, tungsten as seismic mass and stainless steel as housing. Based on the physical prototype, the accelerometer sensitivity is found to be 10 mV/g, mounted resonance frequency is found to be 41 kHz. During the design process, the new design is evaluated and sufficiently optimized by using the Finite Element (FE) simulation before making the actual prototype. Achievement of reasonable agreement between the experi-

mental results of the physical prototype and the simulation results encourages the use of FE modelling for facilitating the design process.

Acknowledgements

Discussions with Knud Styhr Hansen, Lars Munch Kofoed, and Jørgen Stensgaard.

References

[1] M. Serridge and T. R. Licht, *"Piezoelectric Accelerometer and Vibration Preamplifier Handbook, Brüel & Kjær"*, November 1987

[2] ANSYS® user's manual for revision 5.5

[3] S. C. Chen, J. S. Bække and P. Becke, *"IEEE – 1451.4 A Smart Transducer Interface for Sensors and Actuators"* – Mixed-mode Communication Protocols and Transducer Electronic Data Sheet (TEDS) Formats

System for Measurement of Microphone Distortion and Linearity from Medium to Very High Levels

Erling Frederiksen

Abstract

Sound measurements are made over a very wide dynamic range, e.g., from 0 dB to 180 dB. The measurement microphones used are typically calibrated at some level between 70 dB and 124 dB where the existing calibration methods are applicable. Whether calibration at a single level is sufficient is a question raised, not only by aero-space organisations, but also by accreditation bodies and laboratories performing pattern approval of measurement instruments. The doubt is most relevant in relation to higher sound levels where lack of linearity can be expected to occur. Therefore, it was decided that Brüel & Kjær should develop a system for generation of sound pressure over a wide dynamic range which could be used for routine testing of microphones. This paper describes the design and the properties of the resulting system which generates high pressures by a system of tubes with standing waves. The system, which can be set up upon an ordinary laboratory table, can generate levels as high as 174 dB at 500 Hz with low distortion (<1%) and low electrical power.

Résumé

Les mesurages acoustiques sont réalisés sur une gamme dynamique très large, par exemple de 0 dB à 180 dB. Or, les microphones de mesurage utilisés sont généralement étalonnés sur un niveau compris entre 70 dB et 124 dB, là où les méthodes de calibrages existantes sont applicables. Or, beaucoup contestent le caractère satisfaisant d'un étalonnage à un niveau unique, et notamment les centres d'étalonnage accrédités pour les homologations d'instruments et les acteurs de l'industrie aéronautique et aérospatiale. La pertinence de cette réserve est particulièrement sensible dans le cas de niveaux acoustiques élevés, là où le critère de linéarité risque d'être mis à mal. C'est la raison pour laquelle Brüel & Kjær a entrepris de développer un

système d'émission de niveaux de pression acoustique sur une large gamme dynamique, qui serait utilisable pour les vérifications des microphones. Cet article présente la conception et les propriétés d'un tel système, de faible consommation, basé sur la technique des tubes d'ondes stationnaires et qui peut être installé sur une simple table et génère des signaux de pression acoustique jusqu'à 174 dB à 500 Hz sans distorsion notable (<1%).

Zusammenfassung

Schallmessungen erfolgen über einen sehr weiten Dynamikbereich, z.B. von 0 dB bis 180 dB. Messmikrofone werden im Rahmen der üblichen Kalibrierverfahren meist bei einem Pegel zwischen 70 dB und 124 dB kalibriert. Ob die Kalibrierung bei nur einem Pegel ausreichend ist, wird nicht nur von Organisationen der Luft- und Raumfahrt angezweifelt, sondern auch von Akkreditierungsstellen und Laboratorien, die Bauartprüfungen von Messgeräten vornehmen. Die Vorbehalte betreffen besonders die höheren Schallpegel, bei denen Linearitätsverluste zu erwarten sind. Brüel & Kjær hat daher ein System für Routineprüfungen an Mikrofonen entwickelt, das Schalldrücke über einen weiten Dynamikbereich erzeugt. Dieser Artikel beschreibt Bauart und Eigenschaften des Systems, das hohe Schalldrücke durch ein Schlauchsystem mit stehenden Wellen erzeugt. Das System kann auf einem normalen Labortisch aufgestellt werden und erzeugt Pegel bis 174 dB bei 500 Hz mit niedrigem Klirrfaktor (<1%) und geringer elektrischer Leistung.

Introduction

Sound measurements are made over wide frequency and dynamic ranges, exceeding those related to human hearing. Therefore, to ensure valid results, there is a need for calibration methods which cover correspondingly wide ranges. Today, sensitivity- and frequency-response calibrations are based on the free-field and pressure-reciprocity techniques. These methods are highly refined and produce very accurate results from, e.g., 10 Hz to 25 kHz. However, these methods are only applicable within a narrow dynamic range. Therefore, they should be supplemented with an equally precise method for testing dynamic linearity. This is especially needed at high sound levels where lack of microphone linearity can be expected.

This paper describes a method and a system for high-level calibration of various types of measurement microphones. The system is designed to operate at 500 Hz. It can generate pure-tone sound pressures with peak levels as high as

174 dB. The performance of the high-pressure system is monitored and verified using two high-pressure microphones of different design and principle of operation. Harmonic distortion, root-mean-square pressure, and positive and negative peak pressure have been carefully analysed and can be measured with the system.

Methods used for High-pressure Calibration

Most sound-level meters are calibrated at 94 dB or 124 dB but may be used up to 140 dB or 150 dB. Other instruments are used for measurement of sounds from jet engines, fired weapons and launched rockets, which can reach as high as 170 dB to 180 dB. Therefore, the ideal system for high-pressure calibration would have to cover a very wide dynamic range.

Devices for high-pressure generation and calibration have been designed and built by many acoustic laboratories. They are usually low-frequency units and are most often based on the principle of the pistonphone. Some are high-precision sources, like the Laser Pistonphone of the National Physical Laboratory (UK) [Ref. 1], but they are generally designed for operation at one or more levels and are not flexible for wide-range calibration.

The so-called 'pressure-step method' is another method for calibration at high sound pressures. The microphone to be calibrated is placed inside an enclosure, where a known static pressure is established. The calibration step is generated by a sudden release of this pressure which is obtained by breaking a tensioned diaphragm. This method is simple and a good supplement to other methods, but it does not work over a wide pressure range and has been reported to suffer from lack of repeatability [Ref. 2 and 3].

High-pressure calibration systems based on electrodynamic drivers have been built by several laboratories. The high pressure is generally generated inside a cavity where the microphone is placed. High levels are obtained by using small or resonating cavities, tubes with standing waves and, most often, by using high-power speakers or horn drivers. The former Brüel & Kjær High-pressure and Low-frequency Calibrator Type 4221, belongs to this group. It could generate up to 160 dB SPL at 90 Hz, but the product was discontinued as it needed a modern replacement.

New System For High-pressure Generation

Requests for a high-pressure calibration system initiated a project on generation of high sound pressures. The requirements for the new system were that it should preferably work at a commonly used calibration frequency, e.g., 250 Hz, 1000 Hz, or somewhere in between. It should also work up to a peak level of (at least) 170 dB with low distortion and thus produce well-defined root-mean-square and peak pressure. Furthermore, the level of vibration should be low to make the system suitable for calibration of many types of high-pressure microphone. Such microphone types often have a large moving mass and are thus very sensitive to vibration.

It soon became clear that composing a system consisting of a loudspeaker and a resonating system of tubes would be a practical and simple way for obtaining high sound-pressure levels. However, generation of high sound-pressure levels requires high electrical and acoustical power which impose a high driving force on and/or a large displacement of the speaker diaphragm. This can lead to serious, speaker-generated distortion which should ideally be eliminated by the resonating tubes before the sound reaches the position of the microphone under test.

Tube resonance peaks will typically appear at frequencies where a quarter or a half wavelength of the sound equals the length of the tube. The specific ratio of the wavelength and the frequency depend on the impedance terminating the tube.

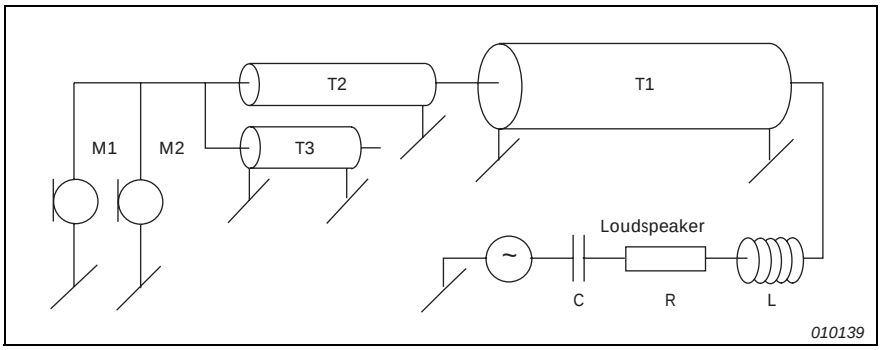

Fig. 1. Simplified model of resonating system of tubes for generation of high sound-pressure levels. The tubes are simulated by transmission lines (T1, T2, T3). The major tubes generate the high pressure, the smaller one reduces distortion

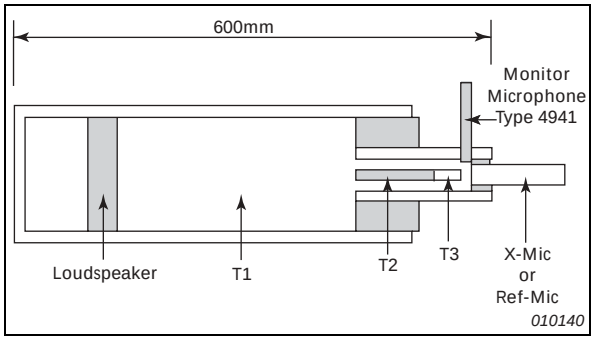

Fig. 2. Sketch of system optimised for operation at 500 Hz. The system consists of 3 tubes (T1, T2, T3). Tube diameters [mm]: 100 (T1), 25 (T2) and 4 (T3). The high sound pressure is generated at the position of the microphones. Microphone under test can be up to Ø 25 mm

When this impedance is significantly higher or lower than the characteristic impedance of the tube, resonance peaks will also appear at frequencies which are either even or uneven multiples of the fundamental resonance frequency. As this may increase distortion, tube dimensions and terminations leading to peaks at harmonic frequencies should definitely be avoided in the design of the system.

Calculations were made with several combinations of coupled tubes of various lengths and diameters by using models like the one shown in Fig. 1. System responses were calculated by using the electrical circuit calculation program, PSPICE, which uses electric transmission lines to simulate the acoustic transmission lines made up by the tubes. After optimisation by simulation, a physical model was built, Fig. 2. Acoustically, the model behaved as expected. Only minor changes were made to obtain the properties of the system described in the following.

The measured response of the final system is shown in Fig. 3. (see curve 'A') which shows that the highest sound pressure is generated at 500 Hz. This is important, because 500 Hz is the system's operating frequency. It also shows that the sound pressure is very low at all harmonic frequencies of 500 Hz. This means that distortion components generated by the loudspeaker are greatly reduced at the microphone position. Having made this design optimisation, it was found that the most dominating component of the remaining distortion was the 3rd harmonic. As this microphone distortion component is related to lack of linearity, it was decided to improve the system performance by implementing an extra tube (T3). Curve 'B', in Fig. 3., shows the response, as it was before the implementation of the tube which reduced the 3rd-harmonic distortion by

about 8 dB. The tube system is designed to create high input impedance at 500 Hz. This implies a relatively low displacement of the loudspeaker diaphragm and a low level of vibration acting on the microphone being calibrated.

Fig. 3. shows the measured frequency response of the system used for generation of high sound levels at 500 Hz. Notice that the level is very high at this frequency compared to those at its harmonics.

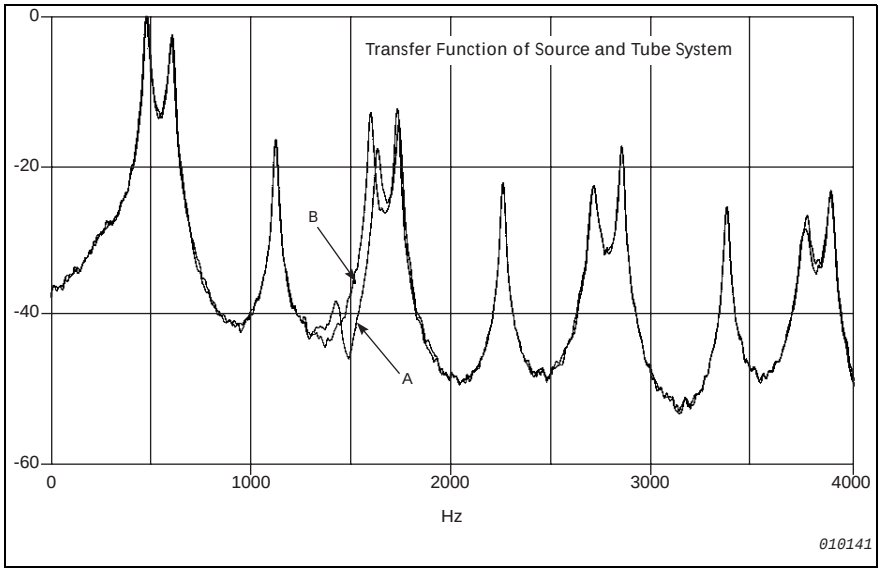

Fig. 3. Measured frequency response of system used for generation of high sound levels at 500 Hz. Curve 'A' shows the final response. Curve 'B' shows the response without the tube for 3rd-harmonic minimisation

Determination And Analysis Of Sound Pressure

The system, consisting of loudspeaker and tubes, can generate high sound-pressure levels but is not considered to be fully linear by itself. In fact, the ratio between generated pressure and input current has not been analysed at all. The reference for system linearity is two high-pressure microphones which comprise part of the system. One is Brüel & Kjær Condenser Microphone Type 4941 which has a small and very stiff diaphragm and sensitivity as low as -81 dB re. 1 V/Pa. The other microphone is Piezoelectric Microphone Type 2510 from ENDEVCO® which has a sensitivity of -90 dB re 1 V/Pa. Both microphones are

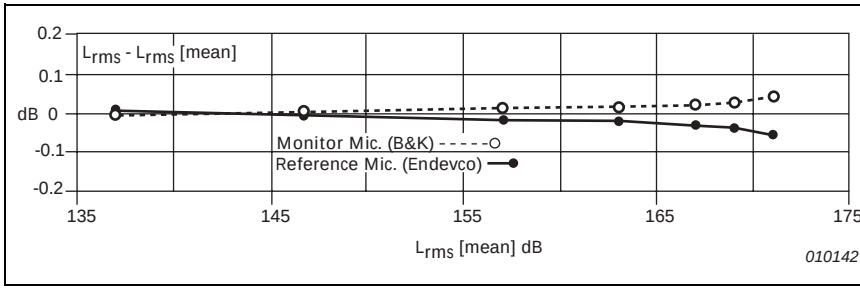

Fig. 4. Measured levels of root-mean-square pressure displayed relative to their mean value

meant to be capable of working up to levels more than 20 dB above the maximum level of the high-pressure system. Therefore, both of them were assumed to be good references for high-level sound pressure but the results obtained with the two microphones were analysed before this was finally confirmed.

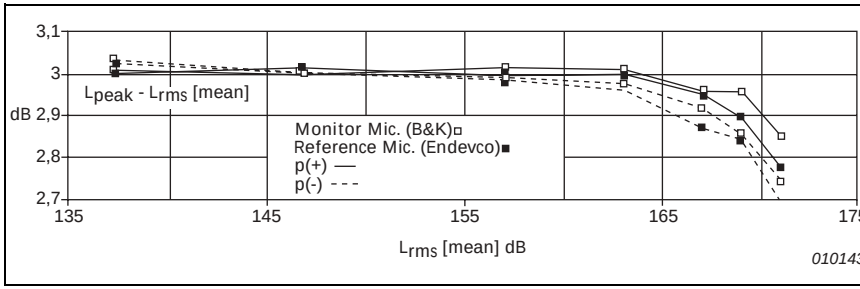

Fig. 5. Measured positive and negative peak pressure levels displayed relative to RMS-level. The peak levels are fully as should be expected up to 164 dB, above which they decrease slightly

The Brüel & Kjær Portable PULSE™ Multi-Analyzer System Type 3560 C was set up as a two-channel analyzer and used for analysis of the microphone output signals at a series of high sound-pressure levels. Fig. 4. shows the root-mean-square values measured by the two microphones. As can be seen, the measured values differ very little below, e.g., 164 dB (rms), above which the difference increases to a little less than 0.1 dB at 170 dB. Fig. 5. shows measured positive and negative peak-pressure levels relative to measured RMS-value of the pressure. At RMS levels below, say, 164 dB, the peak pressure is as should be expected for a sinusoidal signal, namely 3 dB above the level of RMS pressure. At 170 – 171 dB, the peak-pressure level has decreased by 0.2 dB.

The level of harmonic distortion is another measure for linearity or lack of same. Therefore, harmonics from 2nd (1 kHz) to 7th (3.5 kHz) were also measured using both microphone types. The results obtained with the ENDEVCO® Type 2510 microphone are shown in Fig. 6. and those with the Brüel & Kjær Type 4941 in Fig. 7. Both sets of results show very low distortion, especially when the very high sound-pressure levels are taken into account. The results are essentially equal (see Fig. 9.), but there is one exception, namely the 2nd-harmonic component, which is higher in the case of the Brüel & Kjær microphone. However, this was to be expected because condenser microphones tend to produce this type of distortion at high levels. This is especially true when the passive capacitance of the microphone is of the same order of magnitude as the active diaphragm to back-plate capacitance as is generally the case for smaller microphones like Type 4941. This phenomenon is illustrated by the two examples of distortion measurement reported later in this paper. The difference between the results is due to the capacitance loading the microphone in case number two. Therefore, the 2nd-harmonic result obtained with Type 2510 is the better to rely on.

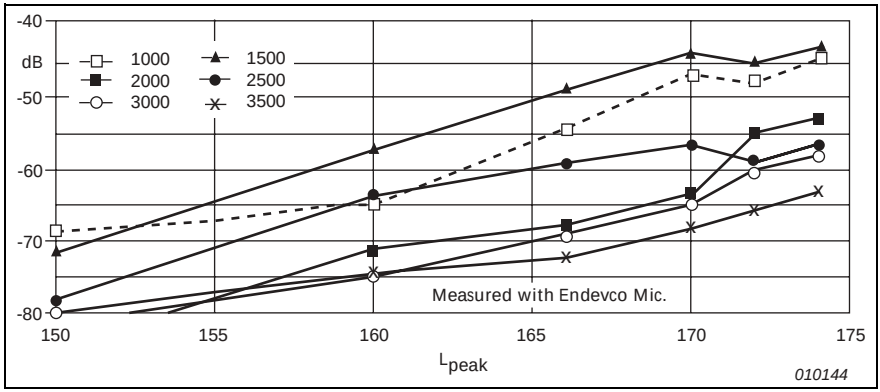

Fig. 6. Harmonic distortion of high-pressure system as measured with Endevco Piezoelectric Microphone Type 2510. The 3rd harmonic is the dominating component, but all components are low and make the total distortion less than 1% at 174 dB

The high-pressure system has been analysed over a wide dynamic range. Generally, the results obtained with the two microphones agree. This agreement is illustrated by Fig. 4., Fig. 5. and Fig. 8.The only exception, the 2nd-harmonic distortion, can be explained. Therefore, when the responses to the high-pressure signals of two different microphones are essentially equal, one must assume that both microphones measure correctly and that they measure the

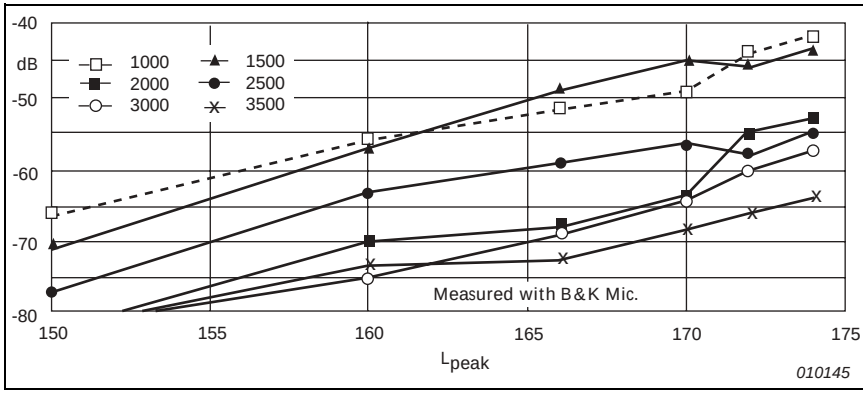

Fig. 7. Harmonic distortion of high-pressure system as measured with Brüel & Kjær Condenser Microphone Type 4941. The result agrees with that found with Type 2510, but the 2nd harmonic is higher. This was to be expected (see explanation in the main text)

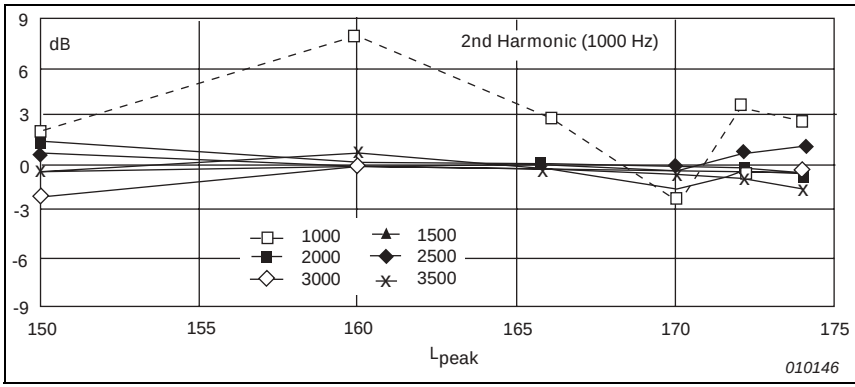

Fig. 8. Difference between the harmonic distortion as measured by the Brüel & Kjær Type 4941 and the Endevco Type 2510. Deviations at 154 dB are due to uncertainty of low distortion results. See main text about 2nd harmonic distortion

true properties of the system. It can, therefore, be concluded that the system can produce pressures of very low distortion and essentially ideal, positive and negative peak levels up to, say, 170 dB peak. Between 170 dB and 174 dB peak, the quality of the produced pressure is only slightly reduced.

Errors of peak level and magnitude of harmonic distortion are very small and several times less for this system than it would have been if the system was

based on the pistonphone principle which generates sound pressure by equall - large, positive and negative volume displacements.

The absolute sound-pressure level was determined by calibrating the high-pressure microphones at 124 dB using a Brüel & Kjær Pistonphone Type 4228. Both microphones will be part of the future system. The ENDEVCO® Piezoelectric microphone Type 2510 will become the reference standard of the system, while the Brüel & Kjær Condenser Microphone Type 4941 is so small that it can be mounted together with the microphone under test and can thus monitor the generated pressure. Prior to any calibration, both microphones can be used for system verification.

Measurement Results Obtained With Brüel & Kjær Pressure-field Half-inch Microphone Type 4192

After the design and test of the system, it was used for linearity and distortion measurement of the Brüel & Kjær half-inch microphone, Type 4192, which has an open circuit sensitivity of 12.5 mV/Pa. The response of this microphone was measured with loading of 0.3 pF and 100 pF. The small capacitance, which represents the normal mode of operation, was made up by the input capacitance of a standard Brüel & Kjær Preamplifier Type 2669. The larger capacitance was that of adapter UC 0211 which is generally used with the same type of preamplifier and microphone Type 4193 for measurement of infra-sound. As microphones Types 4192 and 4193 are equal in all respects, with the exception of time constants of static-pressure equalisation, the distortion results below are valid for both types (see Fig. 9. to Fig. 12. and Fig. 14.). Notice the dramatic decrease in linearity and increase in harmonic distortion which are caused by the larger, parallel capacitance. More can be read about this subject in Brüel & Kjær Technical Review, No. 1 – 1996[Ref. 4].

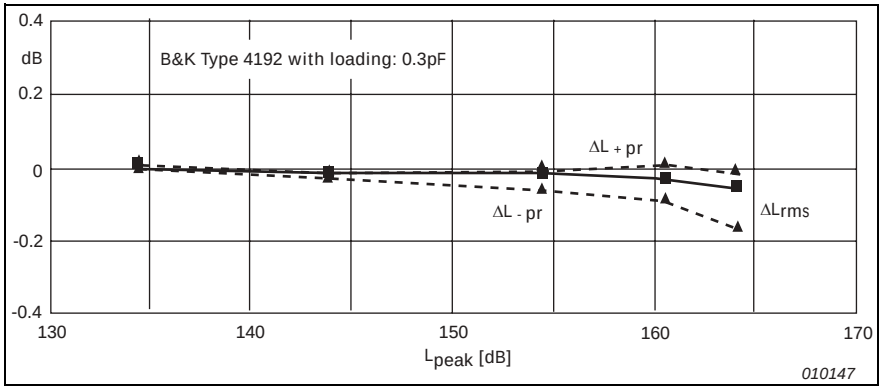

Fig. 9. Linearity of positive and negative peak and RMS levels of Brüel & Kjær Half-inch Microphone Type 4192 and Half-inch Microphone Preamplifier Type 2669

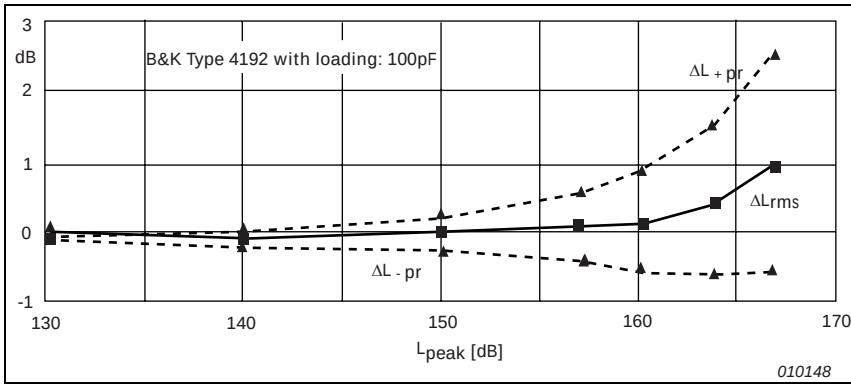

Fig. 10. Same as Fig. 9., but with 100 pF loading of the microphone (UC 0211). Be aware of the large scale difference

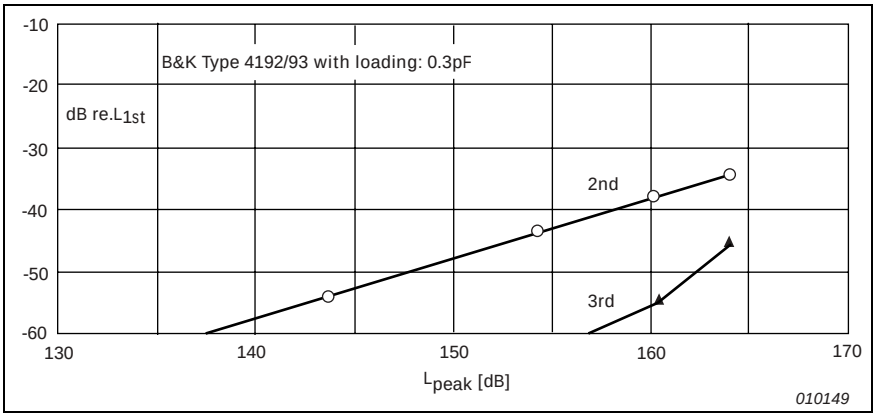

Fig. 11. Harmonic distortion of Brüel & Kjær Half-inch Microphone Type 4192 and Half-inch Preamplifier Type 2669

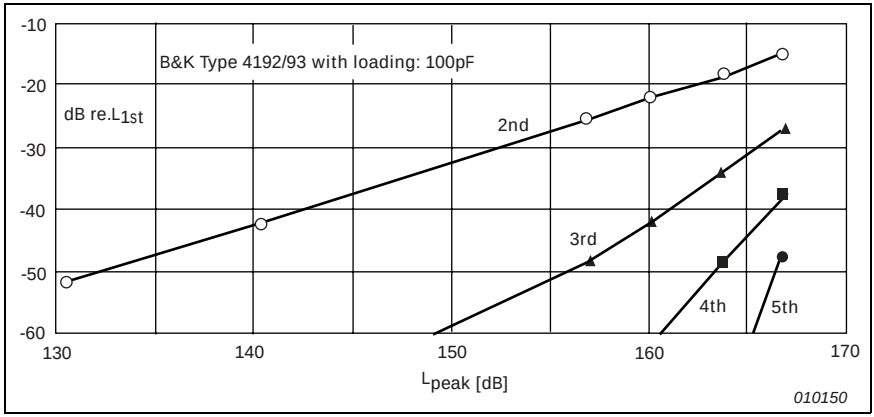

Fig. 12. Same as the above figure, but with 100 pF loading of the microphone (UC 0211)

Fig. 13. Microphones Types 4192 and 4193, and Adaptor UC 0211 (respectively from left)

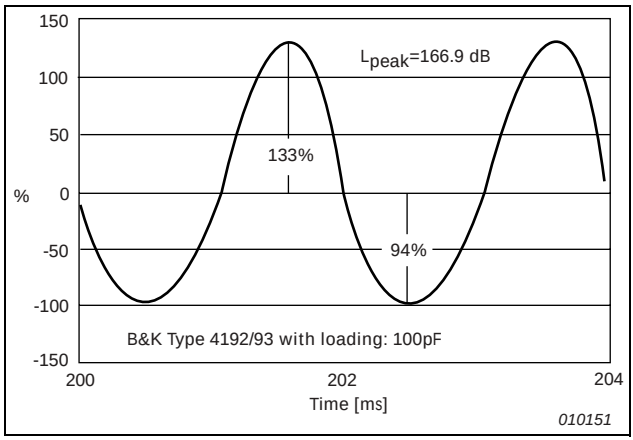

Fig. 14. Instantaneous sound pressure as measured by microphone Type 4192 with UC 0211 (100 pF parallel capacitance). The loading capacitance causes heavy distortion of the microphone output signal and leads to incorrect peak-level measurements. This measurement is made to illustrate influence of loading capacitance only. Brüel & Kjær do not recommend this mode of operation at this high level (167 dB)

Conclusions

A new system has been developed for the generation of medium to very high sound pressures. The system operates at 500 Hz. It generates an essentially pure tone at this frequency which can be applied to microphone analysis with respect to the linearity of peak/root-mean-square pressure, and harmonic distortion. The system can generate peak levels up to 174 dB (0.1 bar) with harmonic distortion less than 1%. The system references of linearity and sound pressure are Endevco Piezoelectric Microphone Type 2510, and Brüel & Kjær Quarter-inch Microphone Type 4941. The results were analyzed by a Brüel & Kjær Portable PULSE™ Multi-analyzer System Type 3560 C which also controlled the measurements. The system's operation frequency can be changed by adjusting the tube-system dimensions or by replacing the air in the system with another gas.

References

[1] D.C. Aldridge, D. R. Jarvis, B. E. Jones, R. T. Rakowski, *"A Method for Demonstrating the Linearity of Measurement Microphones at High Sound Pressures"*, ACUSTICA, 84, 1167 - 1171, (1998)

[2] D.C. Aldridge, D. R. Jarvis, B. E. Jones, R. T. Rakowski, *"Pressure-Step Method for Determining the Low Frequency Sensitivity of Measurement Microphones at High Sound Pressures"*, ACUSTICA, 84, 1161 - 1166, (1998)

[3] A. Hunt, P. Schomer, *"High-amplitude/low-frequency impulse calibration of microphones; a new method"*, J. Acoust. Soc. Am., 65, (1979)

[4] E. Frederiksen, *"Reduction of Non-linear Distortion in Condenser Microphones by Using Negative Load Capacitance"*, Brüel & Kjær Technical Review, No. 1 (1996)

APPENDIX

Hardware Description of System for Testing of Microphones at High Sound Pressure Levels

Erling Frederiksen

This description refers to the paper "*System for Measurement of Microphone Distortion and Linearity from Medium to Very High Levels*", which was given at the ICSV conference in Hong Kong, July 2001. The paper deals with the principle of high-pressure generation and gives examples of measurement results obtained with the system. In the following text, the instruments used will be described in more detail.

The sound pressure is generated by a loudspeaker which is connected to a system of coupled tubes. The design of the unit with the speaker and largest tube originates from the Brüel&Kjær Impedance Measurement Tube Type 4206, while the other tubes are made specifically for the purpose of high-pressure generation. A generator drives the speaker at 500 Hz via a Brüel&Kjær Power Amplifier Type 2706. The output tube, where the high pressure occurs, has two microphone ports. The port in the longitudinal axis accepts microphones up to a diameter of 25 mm. It can be used for either the high-pressure reference microphone, or for the microphone under test. The other port is designed for a smaller (¼"), high-pressure monitor microphone which is flush-mounted on the inner, cylindrical wall of the tube. The close positioning of the ports ensures that there is essentially the same sound pressure at the inserted microphones.

The reference and the monitor microphones are both high-pressure microphones but are very different with respect to operation principle and design. The reference microphone is ceramic (ENDEVCO Type 2510) while the monitor microphone is a condenser microphone (Brüel&Kjær Type 4941). These different microphones are chosen to verify that the system performs properly. When two such different microphones measure almost the same generated pressure, one can assume that both microphones are measuring correctly – see the ICSV paper and the block diagram Fig. A1.

The system has two channels for measurement and analysis of linearity and distortion. A Brüel&Kjær Multi-analyzer System (Portable PULSE™), which includes a PC, is used for the signal analysis. This analyzer measures distortion, and peak and root-mean-square levels simultaneously in both channels. To ensure the best possible high-level properties of the system, high-voltage power supplies were used for the preamplifiers. The reported measurements were made with Brüel&Kjær Measurement Amplifiers Type 2606 which have later been replaced by two of the four channels of Power Supply Type 2829. The applied preamplifiers are Brüel&Kjær Type 2669.

The generator, which drives the loudspeaker, is implemented in the PULSE™ analyzer.

The measurement instruments for the high-level generation system requires very little space. In fact, the system can easily be operated on top of a normal writing table. Even if the pressure inside the tube system is very high, the outside level is low and does not harm the operator who does not need any hearing protection. Due to the short measurement time, the disturbance caused to nearby personnel is negligible. Fig. A2. shows a photograph of the high-pressure calibration chamber which, including a mounting console, is approximately 75 cm tall.

The raw measurement data from the analyzer are shown on the PC screen

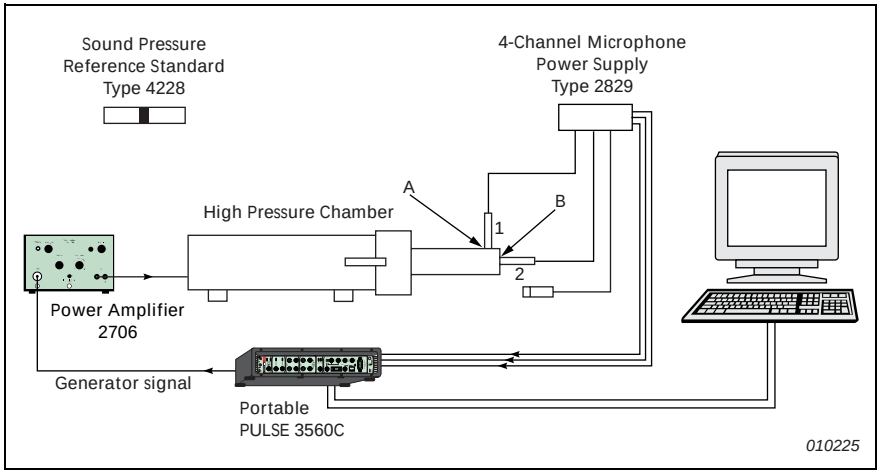

Fig. A1. Measurement setup of high-pressure microphone calibration

(see example in Fig. A3.) and are exported to Microsoft® Excel for the presentation of the final linearity and harmonic distortion results. Software for the auto-

matic control of measurements at different levels and the final presentation of results is under consideration.

Fig. A2. Photograph of the high-pressure calibration chamber

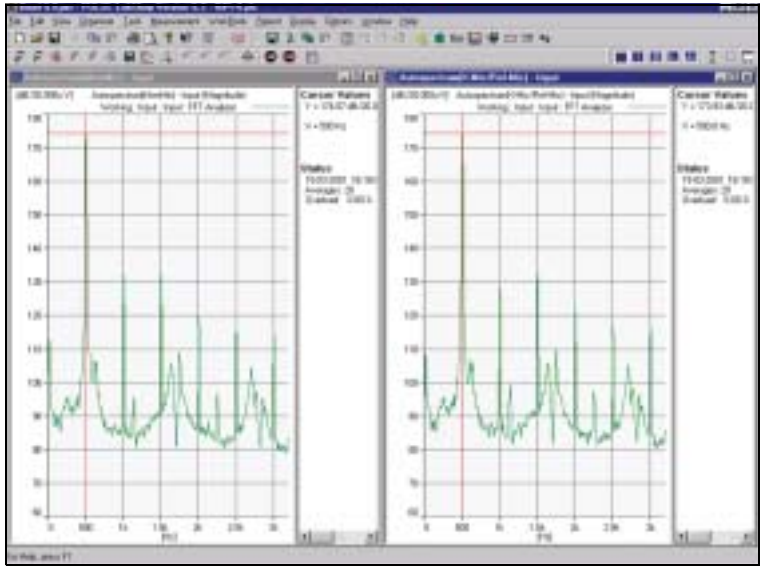

Fig. A3. Autospectra of the pressure measured by the two different high-pressure microphones

Previously issued numbers of Brüel & Kjær Technical Review

(Continued from cover page 2)

1 – 1988 Using Experimental Modal Analysis to Simulate Structural Dynamic Modifications
Use of Operational Deflection Shapes for Noise Control of Discrete Tones
4 – 1987 Windows to FFT Analysis (Part II)
Acoustic Calibrator for Intensity Measurement Systems
3 – 1987 Windows to FFT Analysis (Part I)
2 – 1987 Recent Developments in Accelerometer Design
Trends in Accelerometer Calibration
1 – 1987 Vibration Monitoring of Machines
4 – 1986 Field Measurements of Sound Insulation with a Battery-Operated Intensity Analyzer
Pressure Microphones for Intensity Measurements with Significantly Improved Phase Properties
Measurement of Acoustical Distance between Intensity Probe Microphones
Wind and Turbulence Noise of Turbulence Screen, Nose Cone and Sound Intensity Probe with Wind Screen
3 – 1986 A Method of Determining the Modal Frequencies of Structures with Coupled Modes
Improvement to Monoreference Modal Data by Adding an Oblique Degree of Freedom for the Reference
2 – 1986 Quality in Spectral Match of Photometric Transducers
Guide to Lighting of Urban Areas
1 – 1986 Environmental Noise Measurements

Special technical literature

Brüel & Kjær publishes a variety of technical literature which can be obtained from your local Brüel & Kjær representative.

The following literature is presently available:

- Catalogues (several languages)
- Product Data Sheets (English, German, French,)

Furthermore, back copies of the Technical Review can be supplied as listed above. Older issues may be obtained provided they are still in stock.

BV 0055 – 11 ISSN 0007–2621

HEADQUARTERS: DK-2850 Nærum · Denmark
Telephone: +45 45 80 05 00 · Fax: +45 45 80 14 05
Internet: http://www.bksv.com · e-mail: info@bksv.com

Brüel & Kjær